REPORT DOCUMENTATION PAGE

Form Approved
OMB No. 0704-0188

1. AGENCY USE ONLY (Leave blank)	2. REPORT DATE	3. REPORT TYPE AND DATES COVERED
	November 1995	Final Report 1 Jan 92 - 30 Sept 95

4. TITLE AND SUBTITLE
Theoretical and Numerical Study of Asymmetric Unsteady Lex and Slender-wing Vortices Including Breakdown

5. FUNDING NUMBERS
F49620-92-J-0105

6. AUTHOR(S)
K. Cheung, E. J. Jumper and R. C. Nelson

7. PERFORMING ORGANIZATION NAME(S) AND ADDRESS(ES)
Department of Aerospace & Mechanical Engineering
University of Notre Dame
Notre Dame, IN 46556

AFOSR-TR-96
0372

9. SPONSORING/MONITORING AGENCY NAME(S) AND ADDRESS(ES)
Air Force Office of Scientific Research
110 Duncan Avenue, Suite B115
Bolling AFB, DC 20332-0001

N/A

10. SPONSORING/MONITORING AGENCY REPORT NUMBER
92-J-0105

11. SUPPLEMENTARY NOTES

19960726 059

12a. DISTRIBUTION/AVAILABILITY STATEMENT

UL

Approved for public release,
distribution unlimited

13. ABSTRACT (Maximum 200 words)

The following final report documents the accomplishments made under AFOSR Grant F49620-92-J-0105 for the period starting January 1, 1992 and ending September 30, 1995. During this time, progress was made in better understanding the spiral vortex breakdown phenomenon. A theoretical model of vortex breakdown was developed, illustrating the self-induced, cause-and-effect nature of the breakdown spiral in sustaining its geometry in an adverse pressure field. From this study, a geometric compatibility condition was discovered in the form of a non-dimensional circulation strength. Experiments were conducted to experimentally confirm this geometric compatibility condition. An isolated vortex was subjected to two breakdown-inducing flowfields; the first consisted of a flow obstruction, and the second consisted of a pair of counter-rotating cylinders. The geometric compatibility condition was found to exist for the resulting spiral vortex breakdown from both of the experiments. Three papers were written and presented on this study at several AIAA Applied Aerodynamics conferences, and a journal paper is currently under review. Also, an abstract was submitted in October, 1995 for an AIAA Applied Aerodynamics conference in 1996.

14. SUBJECT TERMS	15. NUMBER OF PAGES
Vortex breakdown, vortex dynamics	11
	16. PRICE CODE

17. SECURITY CLASSIFICATION OF REPORT	18. SECURITY CLASSIFICATION OF THIS PAGE	19. SECURITY CLASSIFICATION OF ABSTRACT	20. LIMITATION OF ABSTRACT
Unclassified	Unclassified	Unclassified	UL

Abstract

The following final report documents the accomplishments made under AFOSR Grant F49620-92-J-0105 for the period starting January 1, 1992 and ending September 30, 1995. During this time, progress was made in better understanding the spiral vortex breakdown phenomenon. A theoretical model of vortex breakdown was developed, illustrating the self-induced, cause-and-effect nature of the breakdown spiral in sustaining its geometry in an adverse pressure field. From this study, a geometric compatibility condition was discovered in the form of a non-dimensional circulation strength. Experiments were conducted to experimentally confirm this geometric compatibility condition. An isolated vortex was subjected to two breakdown-inducing flowfields; the first consisted of a flow obstruction, and the second consisted of a pair of counter-rotating cylinders. The geometric compatibility condition was found to exist for the resulting spiral vortex breakdown from both of the experiments. Three papers were written and presented on this study at several AIAA Applied Aerodynamics conferences, and a journal paper is currently under review. Also, an abstract was submitted in October, 1995 for an AIAA Applied Aerodynamics conference in 1996.

I. Theoretical Study

The results of the theoretical study of spiral vortex breakdown can be found in the paper by Jumper, Nelson, and Cheung [1]. A more detailed treatment, including a computer code listing, can be found in Cheung [2]. Results of the work have also been submitted in paper form to *The Journal of Fluid Mechanics*, and is currently under review.

A vortex-filament model was developed for spiral vortex breakdown based on the experimental observation that the coiling sense of the breakdown spiral was always opposite that of the vortex circulation sense. The model's spiral geometry was based on measurements of the spiral breakdown on delta wings, for example see Figure 1. An illustration of the vortex-filament model is shown in Figure 2. In the model, the

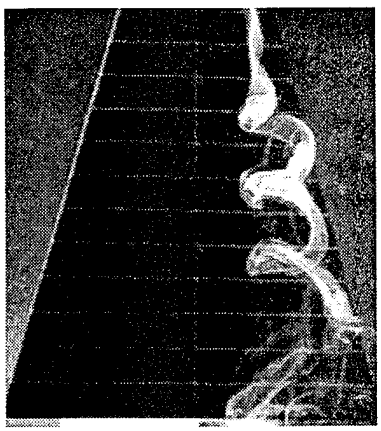

Figure 1: Spiral Vortex Breakdown on Delta Wing

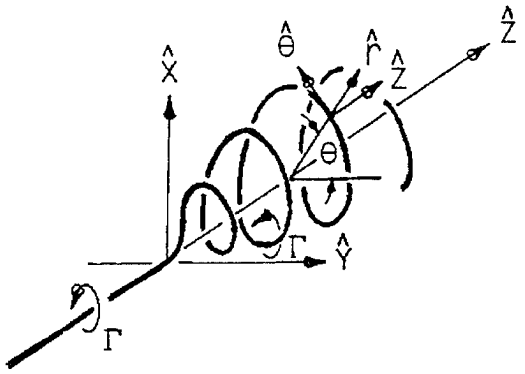

Figure 2: Vortex-Filament Model of Spiral Vortex Breakdown

asymptotic spiral diameter, core diameter, helical pitch, number of revolutions of spiral, and spiral diameter growth rate were extracted from delta-wing flow-visualization experiments. The streamwise and radial velocity components for points that lie *on* the spiral (i.e., self-induced velocity) were numerically integrated, with the result shown in Figure 3, where θ is the spiral generating angle ($\theta = 360°$ corresponds to

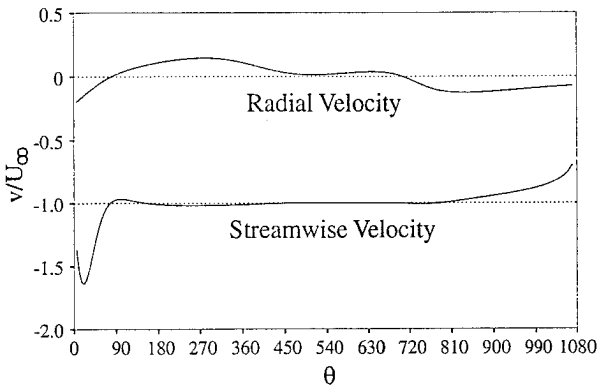

Figure 3: Self-Induced Velocities of Spiral Filament

one revolution of the spiral). Notice that for most of spiral ($\theta > 90°$), the self-induced velocity on the spiral is equal and opposite that of the freestream, indicating that the spiral is stagnated with respect to the wing reference frame. The elevated self-induced velocities at the beginning portion of the spiral is compatible with the observation that there is an axial jetting down the core of the pre-breakdown vortex. This elevated region, then, is necessary to stagnate and divert the extra momentum of the vortex core due to the jetting. The non-dimensional circulation strength for this condition was found to be $\tilde{\Gamma} = \frac{\Gamma}{DU_\infty} = 1.32$, where D is the asymptotic spiral diameter. This was what was termed the "geometric compatibility condition" for spiral vortex breakdown, since it gives a relationship between vortex strength, spiral geometry, and the flowfield velocity needed to be counteracted in order to keep the breakdown in a

stable position with respect to the delta wing reference frame.

The relationship between circulation and delta-wing geometry was established in a correlation developed by Hemsch and Luckring [3] for vortex strength past the trailing edge of a delta wing, verified by Visser [4], [5] to be valid on the delta wing. Using this correlation and the geometric compatibility condition ($\tilde{\Gamma}$), a relationship between angle of attack of the delta wing, chordwise location of breakdown, and delta-wing sweep could be solved for. The result is shown in Figure 4. Except for

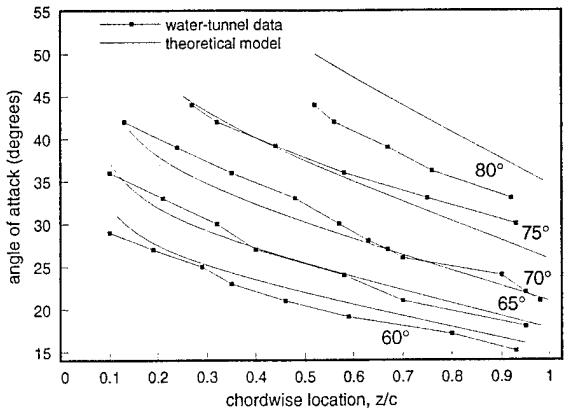

Figure 4: α Versus Breakdown Location

the case where $\Lambda = 80°$ there is good agreement between experiment and the model. The experimental data was available courtesy of Thompson [6].

II. Wind-Tunnel Experiments

With the success of the theoretical model, attention was turned next to verifying the geometric compatibility condition experimentally. A new method of generating a vortex was employed, because although the model incorporated the spiral-breakdown geometry from delta-wing flow-visualization studies, the spiral filament in the model was essentially an isolated vortex. Thus, an experimental setup to more closely match the theoretical model was developed. The isolated vortex was generated by the differential deflection of two adjoining, NACA-009 wing sections. This test section is shown schematically in Figure 5. The vortex is essentially a combination of two wing-tip vortices created at the juncture of the two wing sections. The advantage of generating the vortex in this manner was that the vortex strength could be adjusted independently of the breakdown flowfield. This was not possible for a delta-wing scenario; to adjust the strength for a delta-wing vortex, the wing's angle of attack had to be adjusted.

The isolated vortex just described was caused to break down in two ways. The first was to introduce an obstruction downstream of the vortex generator. Details of this study were presented at the 12^{th} AIAA Applied Aerodynamics Conference at Colorado Springs in 1994 [7]. The second method to induce spiral breakdown was using two counter-rotating cylinders which, together, induce an upstream velocity

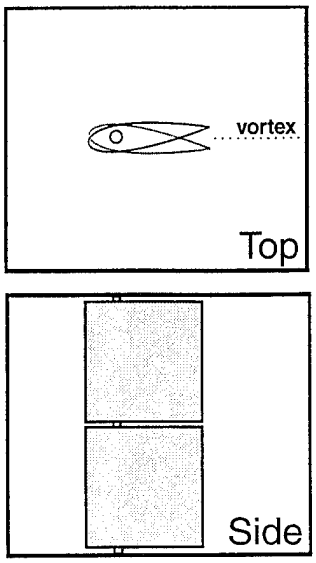

Figure 5: Schematic of Vortex-Generator Test Section

along the vortex axis. The results of this study were presented at the 13^{th} AIAA Applied Aerodynamics Conference at San Diego in 1995 [8]. Results of both studies will be described briefly below.

An illustration of the test sections involved in the flow-obstruction-induced breakdown study is shown in Figure 6. The flow obstruction was a plate inclined to the

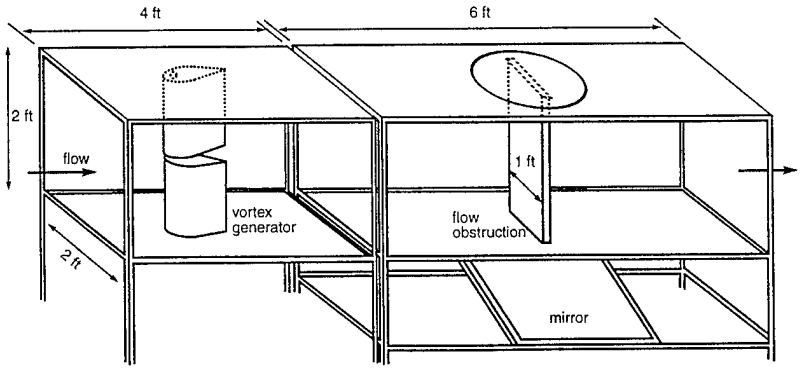

Figure 6: Schematic of Vortex-Generator and Flow-Obstruction Test Sections

freestream direction. Spiral vortex breakdown was induced when the trajectory of the isolated vortex coincided with the stagnation streamtube of the obstruction flowfield, along which the pressure gradient is adverse. If the vortex travelled above or below the stagnation streamline, it encountered an accelerating flow (favorable pressure gradient) and maneuvered around the obstruction without breakdown. Figure 7

shows an example of the spiral breakdown induced by the flow obstruction. Because

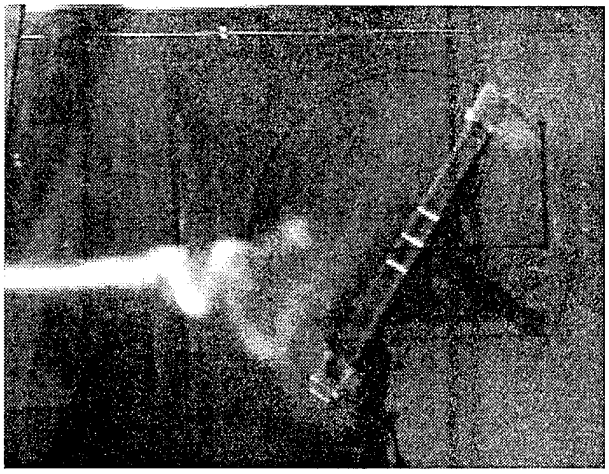

Figure 7: Spiral Vortex Breakdown Induced by Flow Obstruction

the experimental set-up for measuring the vortex strength was still under development, the circulation value was approximated using finite wing theory. Measurement of the obstruction flowfield and characteristic spiral diameter were conducted using graphical analyses (see [7] for details). Using these values, the relationship between $\tilde{\Gamma}$

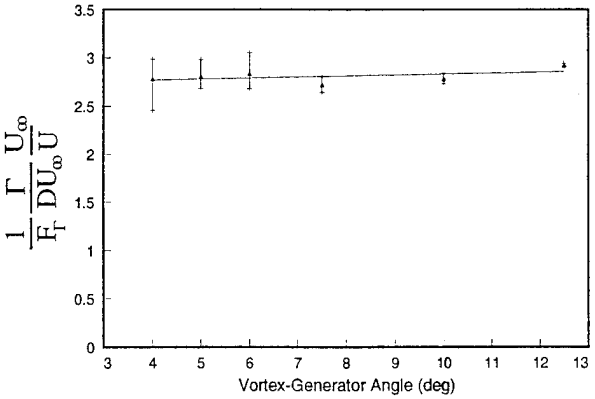

Figure 8: $\tilde{\Gamma}$ Versus Vortex-Generator Angle

and vortex-generator angle (which is equivalent to dimensional circulation strength) was plotted, shown in Figure 8. The velocity used in the non-dimensionalization of circulation for this case was the local velocity; for the theoretical study, the local velocity was estimated to be the freestream velocity. Thus, for this obstruction-induced, spiral-breakdown scenario, a similar geometric compatibility condition discovered in the theoretical model was found to exist.

Finally, the pressure gradient along the vortex trajectory for the externally-imposed flowfield was calculated using the graphical analysis and plotted versus s, the coordinate along the stagnation streamline. The result is shown in Figure 9. Also marked in the figure are the breakdown locations (point where the vortex is disturbed

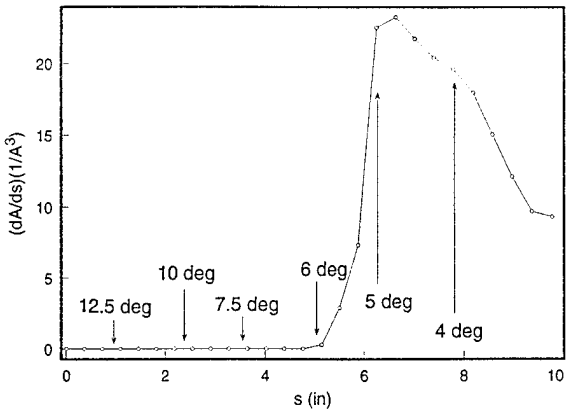

Figure 9: Pressure Gradient Along Vortex Trajectory

from its original trajectory) for different vortex-generator settings. Notice that for some of the settings, the vortex starts to break down in regions of negligible pressure gradient. This supports the claim that after the breakdown process is initiated, the flow stagnation that sustains a stable breakdown position is caused by self induction and not the external flowfield. That is, the breakdown position is well upstream of the event (adverse pressure gradient) that initiated the breakdown process.

The next experimental study was motivated by an attempt to add some sophistication to the breakdown-inducing flowfield. For the flow-obstruction case, there was very limited control of the adverse-pressure-gradient flowfield. In the next experiment, the flow obstruction was replaced by two counter-rotating cylinders that spanned the height of the test section. The cylinders were placed on either side of the vortex and rotated such that they would together induce an upstream velocity along the vortex trajectory. An illustration of the set-up is shown in Figure 10. Control of

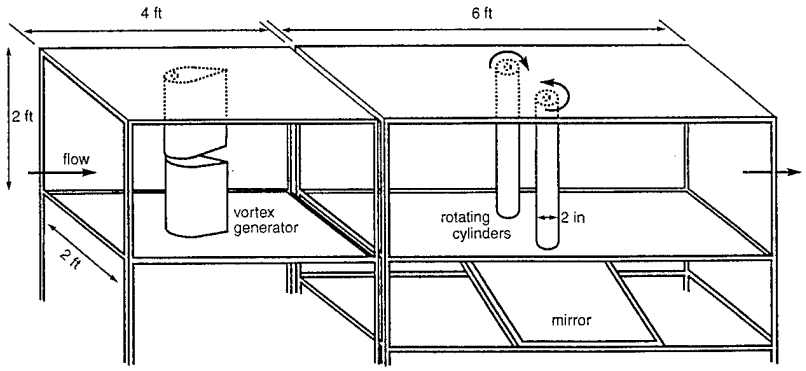

Figure 10: Schematic of Vortex-Generator and Rotating-Cylinder Test Sections

the pressure field could be achieved by the placement, size, and rotation speeds of the cylinders. Details of the experimental procedure, analysis and results can be found in [8].

Measurement of the vortex was performed using a seven-hole-probe (SHP) sys-

tem, designed, constructed and calibrated by Payne [10], following the method of Gallington [9]. The vortex strength was measured in two ways; single, spanwise traverses through the vortex core and two-dimensional wake surveys in the cross-flow plane were performed. Examples of both are shown in Figures 11 and 12, respectively. For the single-traverse method, $\frac{1}{r}$ curves were fit to the azimuthal profiles to identify

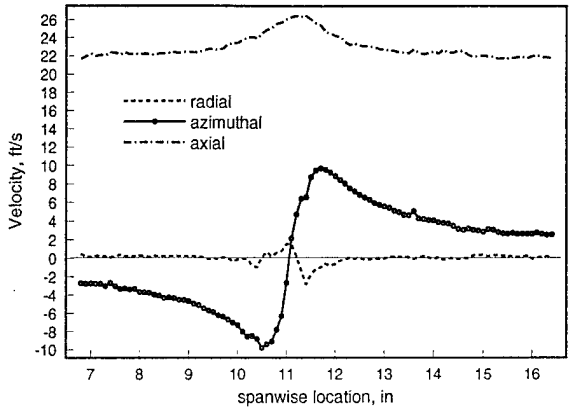

Figure 11: Velocity Components of Single Spanwise Traverse Through Vortex Core

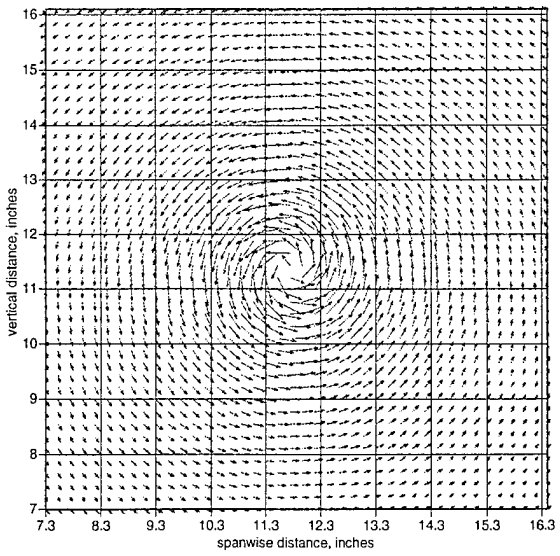

Figure 12: Wake Survey of Vortex FlowField

the vortex "core" size and circulation value. For the wake-survey method, the integral $\int \vec{v} \cdot d\vec{s}$ could be evaluated for varying circular circuits centered about the center of the core to give circulation values. Both methods showed that the circulation continued to increase even at $r = 4.5in$, while the azimuthal profile peaked at $r = 1in$. Since the breakdown spiral is contained well within this region of rotationality, exactly which value of circulation was significant in considering the self-induction of the vortex remained unclear. Thus, upper and lower limits of the vortex strength were established instead.

The streamwise velocity along the vortex trajectory (i.e., between the cylinder pair) was measured using a Pitot-static tube. An example is shown in Figure 13. The velocity is plotted versus ξ, an axis starting at zero directly between the cylin-

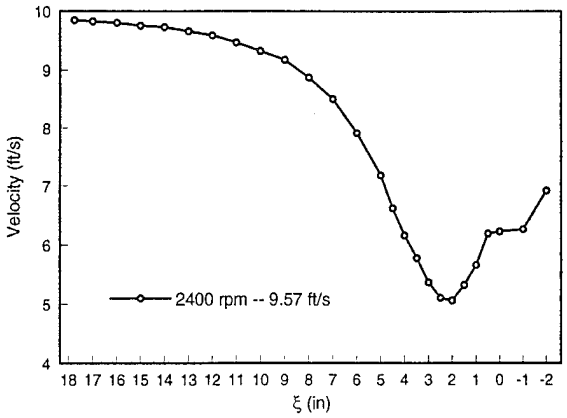

Figure 13: Externally-Imposed Flowfield Velocity

ders and increasing in the upstream direction, coinciding with the vortex trajectory. Notice that there is initially a flow deceleration (adverse pressure gradient) and then a flow acceleration (favorable pressure gradient) just upstream of the cylinders. The magnitude of the pressure gradient was varied by adjusting the rotation speeds of the cylinders.

Spiral breakdown induced by the rotating-cylinder set-up is shown in Figure 14. As was the case in both the delta-wing and flow-obstruction-induced breakdown cases, the sense of the spiral winding was opposite that of the circulation sense. Measurement of the spiral diameter was performed using graphical analysis. Fiducial

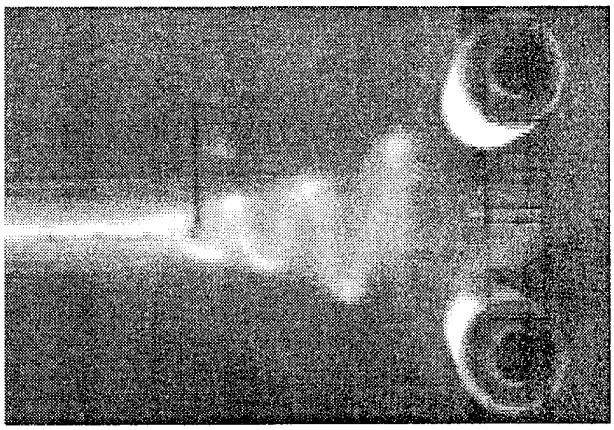

Figure 14: Spiral Vortex Breakdown Induced by Rotating Cylinders

marks were placed on the floor and the ceiling of the test section so that spiral size could be measured by comparison. An example of this measurement is shown in Figure 15. Because it was not obvious whether or not the smoke in the flow visualization

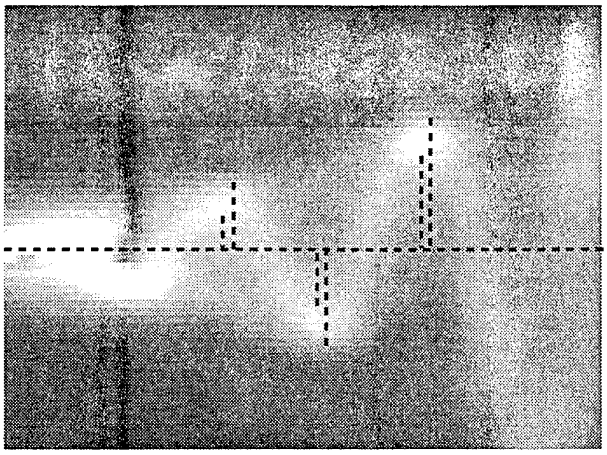

Figure 15: Measurement of Spiral Diameter

marked the precise boundary of the vortex core, measurement of the spiral diameter was performed in such a way as to reduce subjectivity in determining the "location" of the vortex core. An example of the measurement of D is shown in Figure 15, which is a closeup of an image with the same flow conditions as Figure 14. After placing a nominal centerline along the vortex axis, both the top and bottom edges of the spiral peaks were measured, giving an upper and lower bound on the position of the core's center. These lengths were then doubled to give the local spiral diameter for that particular streamwise position, which is measured relative to the cylinders' streamwise placement, i.e., where ξ is defined to be zero. Note that some "systematic" scatter is imposed on a measurement of a diameter above the centerline by the selection of the "nominal centerline;" however, this is imposed in the opposite sense on the diameter measurement made below the centerline.

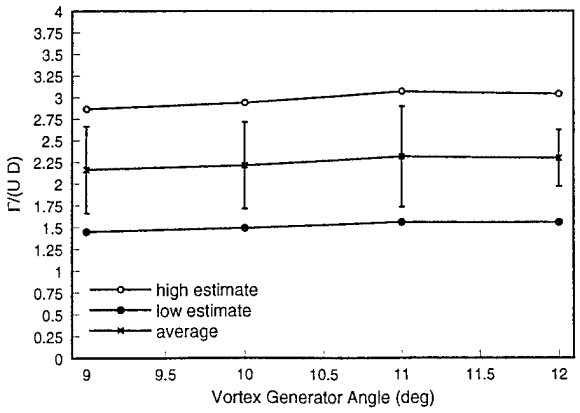

Figure 16: $\tilde{\Gamma}$ Versus Vortex-Generator Angle

Finally, the non-dimensional expression, $\frac{\tilde{\Gamma}}{DU}$, was plotted versus several vortex-generator angles. The result for one flow condition is shown in Figure 16. Included in the figure are measurement uncertainties, as well as the upper and lower bounds

resulting from the circulation measurement. Notice that for the different generator settings (different dimensional circulation values), the non-dimensional circulation is a single value.

Another interesting result that was found was that for lower cylinder-rotation rates, the spiral was first initiated, its position self-sustained, but then the spiral was suppressed by the favorable pressure gradient of the externally-imposed flowfield by stretching the coil in the axial direction. This stretching realigns the negative azimuthal vorticity formed in the spiral into axial vorticity, eventually reforming an axial vortex, albeit apparently with a more diffused core. An image of this is shown in Figure 17. This type of breakdown was termed "psuedo"-spiral breakdown because

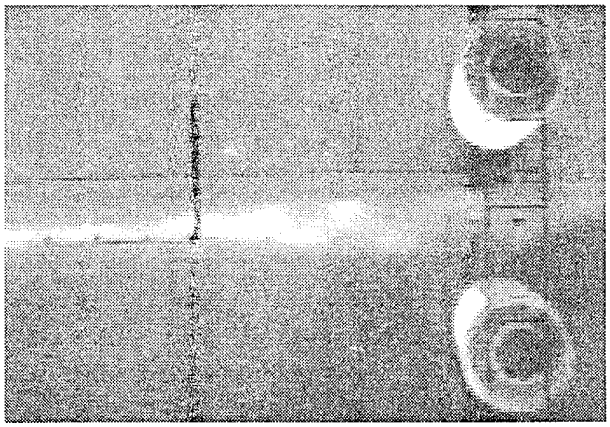

Figure 17: "Pseudo"-Spiral Breakdown

for conventional breakdown, the organized vortical structure of the vortex core is eventually disrupted into turbulence.

The study described above provided further support for the supposition that a "universal" geometric compatibility criterion exists that relates the geometry of the breakdown spiral to the vortex strength so that the requirement to self-perpetuate and sustain spiral vortex breakdown is met. Unlike previous studies, this study provided a quantitative measure for the criterion in the form of a non-dimensional circulation strength, $\tilde{\Gamma}$, equal to approximately 2.25; earlier studies were only able to infer the value of this parameter from theoretical considerations. Of as much interest is the fact that when the breakdown is allowed to pass through the gradient-producing cylinders the spiral can be suppressed and an axial vortex re-established. This suggests that the spiral configuration of the "breakdown" is not, in and of itself, unstable. Rather, the spiral appears to be a stable mode of the vortex, initiated by its own induced upstream jetting, impinging on the pre-breakdown axial vortex, that forces it to kink and begin the spiral. Once formed, the spiral geometry maintains the spiral at its axial location by self-inducing an upstream velocity sufficient to counter the externally-imposed downstream convective flow. The spiral undergoes "full" breakdown only when the imposed flow field *well downstream of the breakdown onset point* forces the final disorganization of the vortex.

References

[1] Jumper, E. J., Nelson, R. C., and Cheung, K., "A Simple Criterion for Vortex Breakdown," AIAA-93-0866 (Applied Aerodynamics Conference), 1993.

[2] Cheung, Ken C.K., "A Theoretical and Experimental Investigation of Vortex Breakdown," *Master's Thesis*, University of Notre Dame, April 1993.

[3] Hemsch, M. and Luckring, J., "Connection Between Leading-Edge Sweep, Vortex Lift, and Vortex Strength for Delta Wings," *Journal of Aircraft*, Engineering Notes, May 1990.

[4] Visser, K. D., "An Experimental Analysis of Critical Factors Involved in the Breakdown Process of Leading Edge Vortex Flows," *Ph.D. Dissertation*, University of Notre Dame, 1991.

[5] Visser, K. D. and Nelson, R. C., "Measurements of Circulation and Vorticity in the Leading-Edge Vortex of a Delta Wing," *AIAA Journal*, Volu. 31, No. 1, January 1993.

[6] Thompson, D. H., Australian Defense Scientific Service Aero. Research Laboratories Note 356, May 1975.

[7] Cheung, K., Jumper, E. J., and Nelson, R. C., "An Experimental Investigation of Spiral Vortex Breakdown," AIAA-94-1880 (Applied Aerodynamics Conference), 1994.

[8] Cheung, K., Jumper, E. J., and Nelson, R. C., "Quantitative, Experimental Investigation of a Geometric Compatibility Criterion in Spiral Vortex Breakdown," AIAA-95-1796 (Applied Aerodynamics Conference), 1995.

[9] Gallington, R. W., "Measurement of Very Large Flow Angles With Non-Nulling Seven-Hole Probes," USAF-TR-80-17, 1980.

[10] Payne, F. M., "The Structure of Leading Edge Vortex Flows Including Vortex Breakdown," Ph.D. Dissertation, University of Notre Dame, 1987.